JEM Journal of Experimental Medicine

BRIEF DEFINITIVE REPORT

Intestinal CD8αα IELs derived from two distinct thymic precursors have staggered ontogeny

Roland Ruscher, S. Thera Lee, Oscar C. Salgado, Elise R. Breed, Sara H. Osum, and Kristin A. Hogquist

CD8αα intraepithelial lymphocytes (IELs) are abundant T cells that protect the gut epithelium. Their thymic precursors (IELps) include PD-1⁺ type A and Tbet⁺ type B populations, which differ in their antigen-receptor specificities. To better understand CD8αα IEL ontogeny, we performed "time-stamp" fate mapping experiments and observed that it seeds the intestine predominantly during a narrow time window in early life. Adoptively transferred IELps parked better in the intestines of young mice than in adults. In young mice, both type A and type B IELps had an S1PR1⁺ and α4β7⁺ emigration- and mucosal-homing competent phenotype, while this was restricted to type A IELps in adults. Only CD8αα IELs established in early life were enriched in cells bearing type B IELp TCR usage. Together, our results suggest that the young intestine facilitates CD8αα IEL establishment and that early IELs are distinct from IELs established after this initial wave. These data provide novel insight into the ontogeny of CD8αα IELs.

Introduction

Intestinal intraepithelial lymphocytes (IELs) are a heterogeneous population of immune cells localized in the epithelium of the gut. They are generally thought to patrol the intestinal epithelium and provide barrier protection and have recently been implicated in metabolism and cardiovascular disease (Cheroutre et al., 2011; He et al., 2019; Hoytema van Konijnenburg et al., 2017; McDonald et al., 2018). The major subsets of IELs are TCRγδ⁺ and TCRαβ⁺ T cells, with the latter composed of induced memory CD4⁺ and CD8αβ⁺ IELs as well as natural CD8α⁺CD8β⁻ (CD8αα) IELs (Cheroutre et al., 2011). CD8αα IELs are derived from thymic IEL precursors (IELps; Gangadharan et al., 2006; Guy-Grand et al., 2013; Lambolez et al., 2006; Pobezinsky et al., 2012; Ruscher et al., 2017), and in recent years, their developmental features have been elucidated in more depth. We and others presented evidence for the existence of two distinct thymic precursor populations (Golec et al., 2017; Ruscher et al., 2017). The dominant population (type A) is self-reactive and PD-1⁺, while a smaller Tbet⁺ population (type B) can be distinguished by expression of CD103, NK1.1, and CXCR3 and may consist of non–self-reactive cells (Ruscher et al., 2017).

Despite recent advances in our understanding of thymic IELps in adults, little is known about IEL establishment in early life. In mice and humans, the intestinal environment undergoes rapid changes, especially between birth and weaning, starting with the ingestion of milk and followed by colonization with bacteria and uptake of solid food (Knoop et al., 2017; Koenig et al., 2011). Therefore, it is important to gain a better understanding of immune cells, particularly CD8αα IELs, at various stages of life. While the IEL compartment is established in mice in the first weeks of life, thymic IELps continue to be generated through adulthood (Gangadharan et al., 2006; Golec et al., 2017; Klose et al., 2018; Kuo et al., 2001; Pobezinsky et al., 2012; Ruscher et al., 2017; Steege et al., 1997). The extent to which IELps continuously seed the gut throughout life is not known. In this study, we aimed to better understand the temporal pattern by which IELps populate the intestine of mice, using a recent "time-stamp" approach. We also sought to shed light on whether different subsets of IELps seed the gut concurrently or asynchronously.

Our data suggest that IELps seed the intestine in a tightly time-restricted wave early in life and that IEL seeding thereafter decreases dramatically. Additionally, in young mice, both type A and type B IELps appear to emigrate and seed the intestine, while in adult mice it is predominantly type A.

Results and discussion

Time-stamping a wave of IELps in adult and neonatal mice

To learn about establishment of CD8αα IELs in an ontogenic context, we first assessed CD8αα and CD8αβ IEL numbers in the

Center for Immunology and Department of Laboratory Medicine and Pathology, University of Minnesota, Minneapolis, MN.

Correspondence to Kristin A. Hogquist: hogqu001@umn.edu; R. Ruscher's present address is Australian Institute of Tropical Health and Medicine, James Cook University, Cairns, Queensland, Australia.

small intestine at various ages. While hardly detectable at younger ages, CD8αα IELs could be detected in the intestine of young animals at 15 d of age and increased to homeostatic levels by 5 wk of age (Fig. S1). This is in agreement with previous publications (Klose et al., 2018; Steege et al., 1997). By 15 d of age, CD8αβ IELs were already present at 10 times higher numbers than CD8αα IELs. Similarly, thymic IELps were present as early as week 2 and continued to be produced throughout adulthood (Golec et al., 2017; Klose et al., 2018; Pobezinsky et al., 2012; Ruscher et al., 2017; Steege et al., 1997). Nonetheless, it was unclear whether the seeding of the intestinal tissue by thymic precursors is constant or not.

To investigate the temporal dynamics of IEL seeding, we employed a so-called time-stamp approach. This approach employs *Cd4*^{CreERT2} crossed with *Rosa26*^{tdT} (stop-floxed tdTomato) mice, in which a floxed-stop cassette preceding the Tomato reporter gene is excised in CD4-expressing cells upon administration of the hormone drug tamoxifen or its metabolite 4-OHT. Since thymocytes go through a CD4$^+$CD8$^+$ double-positive (DP) stage during their development, they are permanently labeled as Tomato$^+$ cells at the DP stage during their exposure to tamoxifen/4-OHT. Therefore, a short pulse of tamoxifen labels a cohort of developing CD8$^+$ T cells (including TCRαβ$^+$ CD8αα and CD8αβ IELs) that were DP thymocytes at the time of exposure to tamoxifen. CD8$^+$ T cells that developed before or after tamoxifen exposure remain unlabeled. This approach allows one to track the fate of CD8$^+$ T cells that developed at a specific developmental window (Smith et al., 2018).

We first sought to establish the labeling kinetics in the thymus of adult versus young mice. In adult animals given a single injection of tamoxifen, we observed a sharp increase in Tomato$^+$ thymocytes by day 2 after administration, which declined by day 5–6 (Fig. S2 A). In neonatal mice, however, after a single weight-adjusted dose of tamoxifen, the proportion of Tomato$^+$ thymocytes continued to increase until day 5–6 after administration. We reasoned that young mice may not have the capacity to process tamoxifen to its active metabolite 4-OHT as efficiently as adult mice, resulting in a slower tamoxifen to 4-OHT conversion and longer bioavailability of 4-OHT in young animals. To get around this issue, we tested the effect of 4-OHT in young animals: after 4-OHT administration into neonatal mice, the resulting peak of Tomato$^+$ thymocytes was nearly identical to that of tamoxifen in adult mice (Fig. S2 A). Hence, in subsequent experiments, we used 4-OHT for young animals.

Upon hormone injection into 7-d-old mice, cells expressing either intermediate (Int) or high levels of Tomato were observed in the thymus. The Tomato^{Int} population was largely composed of CD4$^+$CD8$^+$ DP thymocytes (Fig. S2, B and C). It was prominent at day 2, waned by day 5, and was absent by day 8 (Fig. S2 B), suggesting that these are cells that recently initiated Tomato expression. In contrast, a small Tomato^{High} population was present at day 2 and increased in relative proportion by day 5, then reduced by day 8 (Fig. S2 B). At 2 d after 4-OHT, Tomato^{High} cells were largely CD4SP and expressed the maturation marker H-2K^b (Fig. S2, B and C), likely reflecting mature CD4SPs that were labeled at the time of injection, whereas Tomato^{High} CD8SPs were not present at day 2, were present by day 5, and increased in proportion by day 8 (Fig. S2 C). This pattern reflects that mature CD8 T cells developed from labeled DP thymocytes and emigrated from the thymus within 5–8 d of the time-stamp, consistent with previously established kinetic properties of thymocyte maturation and emigration (McCaughtry et al., 2007). Furthermore, the decline of Tomato^{High} T cells between 5 and 8 d after 4-OHT (Fig. S2 B) is consistent with the majority of mature time-stamp–labeled T cells exiting the thymus in this time span.

Thymic IELps contribute to intestinal CD8αα IELs predominantly in early life

To understand when thymic IELps seed the gut, we time-stamped mice at various ages by giving them hormones at 5, 12, 15, or 21–26 d or as adults (11–16 wk of age; Fig. 1 A). Tomato$^+$ cells within the gut IEL compartment (gating strategy; Fig. S3 A) were enumerated after 4–5 wk—in other words, in adult mice. This approach enabled us to compare IEL establishment in young and adult mice, while allowing for an identical time for each to develop. CD8αα IELs from adult animals showed the highest proportion of Tomato$^+$ cells when hormone was injected at 12 d of age, with a sharp decline thereafter (Fig. 1 B). CD8αβ IELs followed a similar pattern (Fig. 1 C), although with a more gradual decline. As such a rapid shutdown of IEL influx was unexpected, we compared splenic CD8 T cells at similar ages. Indeed, Tomato$^+$ CD8 T cells in the spleen declined less rapidly than CD8αα or CD8αβ IELs (Fig. 1 D), and in adult time-stamped animals, there were substantially more CD8 T cells seeding the spleen than the gut (Fig. 1 E). Importantly, the absolute number of CD8αα IELs 4–5 wk after time-stamping was similar (Fig. 1 F). These data suggest that thymic precursors contribute to the gut IEL compartment most intensely in the neonatal period, with relatively little contribution in adults.

Beneficial conditions for CD8αα IEL establishment in young mice

The high fraction of Tomato-labeled cells in the IEL compartment early in life could reflect enhanced seeding of the gut during the neonatal period, or enhanced proliferation of gut homing cells to "fill the niche" in young mice, or both. Thus, we examined Ki67 expression. Both CD8αα and CD8αβ IELs showed a high fraction of Ki67$^+$ cells between the ages of 15 d and 21 d, compared with a very low fraction of Ki67$^+$ cells in adults (Fig. 1 G). Likewise, the number of IELs was increasing in this same period (Fig. S1). Thus, we conclude that the proliferative activity of IELs is high in young mice. However, Ki67 was high in splenic CD8$^+$ T cells at 15–21 d of age as well (Fig. 1 H), suggesting that additional factors must account for the low contribution of thymic precursors to the IEL pool in adults.

Factors beyond proliferation could additionally account for IEL establishment. We next wanted to establish whether the intestinal environment of young mice might be more receptive to IEL seeding than that of adult mice. To test this for CD8αα IELs, we adoptively transferred thymic CD4$^-$CD8$^-$ (DN) cells, which include mature precursors of CD8αα IELs, into congenically distinct 15-d-old or adult recipients (Fig. 2 A). 4–5 wk after transfer, we recovered more CD8αα IELs from young recipients

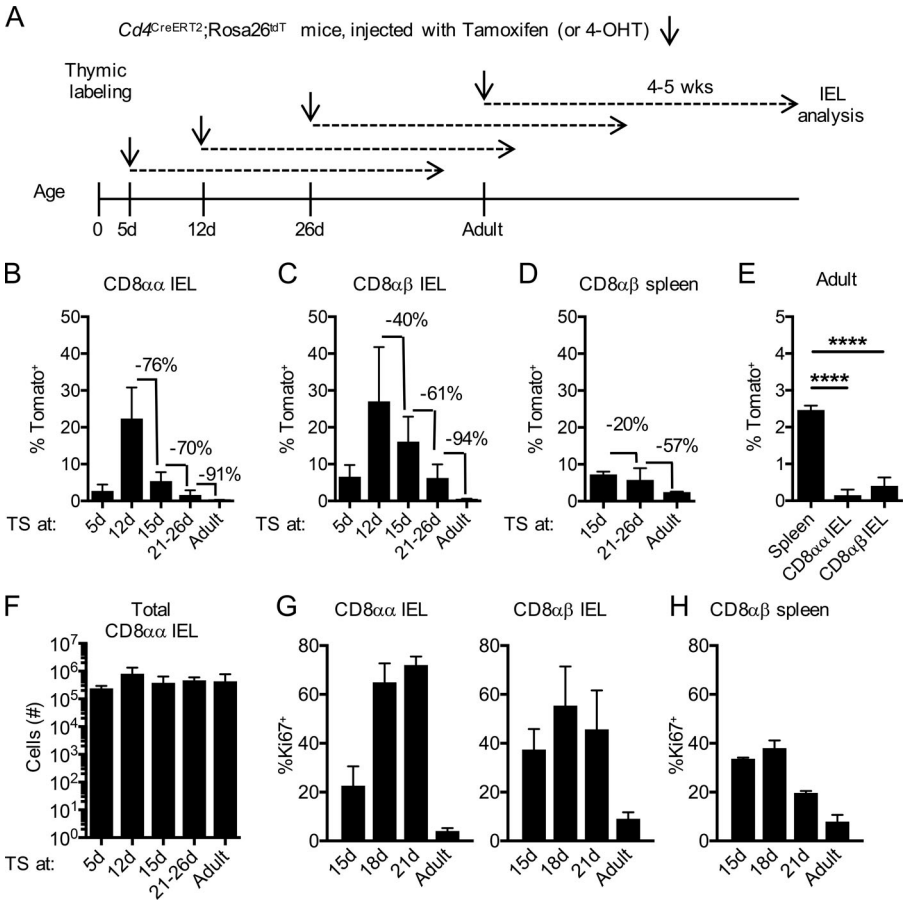

Figure 1. **Thymic IELps contribute to intestinal CD8αα IELs in early life. (A)** Experimental outline: *Cd4*^{CreERT2}×*Rosa26*^{tdT} mice were time-stamped by intraperitoneal injection of tamoxifen (ages 21 d and older) or 4-OHT (ages 5–15 d). Tissues were analyzed 4–5 wk later by flow cytometry. **(B–D)** Frequency of Tomato-labeled cells within small intestinal TCRαβ$^+$ CD8αα (B) or CD8αβ (C) IELs (n = 3 [5 d and 12 d]; n = 8 [15 d]; n = 6 [21–26 d and adult]) or CD8αβ$^+$ T cells (D) in the spleen (n = 3 [15 d and adult]; n = 6 [21–26 d]) in animals time-stamped at the indicated ages. **(E)** Frequency of Tomato-labeled cells in the spleen (n = 3) or IELs (n = 6) of mice time-stamped as adults. **(F)** Numbers of CD8αα IELs in the small intestine at various ages (n = 3 [5 d and 12 d]; n = 8 [15 d]; n = 6 [21–26 d and adult]). **(G)** Frequency of Ki67$^+$ cells within the CD8αα IELs and CD8αβ IELs at various ages (n = 5 [15 d]; n = 4 [18 d and 21 d]; n = 8 [adult]). **(H)** Frequency of Ki67$^+$ cells within CD8αβ$^+$ T cells in the spleen at various ages (n = 5 [15 d and 21 d]; n = 3 [18 d and adult]). Data in B–H are pooled from at least two independent experiments and show the mean ± SD. **(E)** ****P < 0.0001 (ANOVA with Bonferroni post-test). TS, time-stamped.

than from adult mice (Fig. 2 B). The thymic DN population further contains TCRγδ$^+$ T cells. We therefore used TCRγδ IELs as an internal control and compared their numbers with those of CD8αα IELs. Contrary to CD8αα IELs, we observed only a slight difference in donor-derived TCRγδ IEL numbers recovered from 15-d-old and adult WT recipients. Our data therefore suggest that young mice have an inherently greater capacity for CD8αα IEL establishment than adult mice do. This may be a result of greater availability of growth and survival factors such as IL-15, vitamin D, or the CD8αα ligand thymus leukemia antigen due to the relative absence of competing IELs in the gut of 15-d-old mice. This is consistent with the observation that transfer of IELps into RAG2-deficient recipient mice also allows robust recovery of CD8αα IELs (Gangadharan et al., 2006; Klose et al., 2018; Ruscher et al., 2017).

Contrary to those in adults, early-life thymic type B IELps have an emigrating phenotype

Within DN CD5$^+$TCRαβ$^+$ thymocytes of adult mice, "classic" self-reactive (type A) IELps have been identified as PD-1$^+$ cells (McDonald et al., 2014; Ruscher et al., 2017). In addition, we and others discovered a PD-1$^-$Tbet$^+$ (type B) IELp population within DN CD5$^+$TCRαβ$^+$ thymocytes (Klose et al., 2018; Ruscher et al., 2017). To gain a better understanding of IEL ontogeny, we characterized IELps in neonatal and young mice. While hardly detectable in 7-d-old animals (not shown), a sizable population of IELps was found in the thymus by 15–18 d after birth—a time that coincides with the estimated peak influx into the gut in our time-stamp experiments (taking into account the 5–8-d delay in thymic emigration after labeling). Further, mature-phenotype IELps were already composed of PD-1–expressing type A cells as well as PD-1$^-$Tbet$^+$ type B cells in 15-d-old animals (Fig. 3 A). The gating strategy for mature IELps is shown in Fig. S3 B.

We previously reported that type A IELps were the predominant population emigrating from the thymus in adult mice. About 10 times more type A than type B IELps emigrate from the adult thymus, despite their equal proportions within the thymus (Ruscher et al., 2017). Accordingly, type A but not type B IELps showed concomitant KLF2 and S1PR1 expression (Fig. 3 C; Ruscher et al., 2017), which is required for thymic emigration into the bloodstream (Carlson et al., 2006; Matloubian et al., 2004). Contrary to those of adult animals, type B IELp cells from young animals expressed KLF2 and S1PR1 to a similar extent as type A IELps (Fig. 3, B and C). On the other hand, the integrin CD103 (also known as α_E) has been associated with cell retention mediated by binding E-cadherin expressed by epithelial cells, including thymic epithelial cells (Cepek et al., 1994; Kutlesa et al., 2002; Schon et al., 1999). While type B IELps in adult mice are strongly CD103$^+$, they expressed little CD103 at 15 d of age (Fig. 3, D and E). Finally, type A IELps in adults selectively expressed the integrin $\alpha_4\beta_7$ (Fig. 3, F and G; Ruscher et al., 2017), which plays a role in homing to mucosal tissues (Berlin et al., 1993; Hamann et al., 1994). Again, contrary to those of adult animals, the type B IELps in the thymus of 15-d-old mice

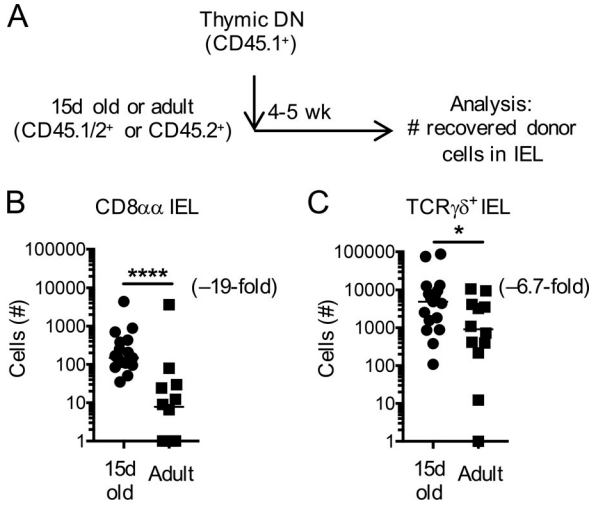

Figure 2. **Beneficial conditions for CD8αα IEL establishment in early life. (A)** Experimental outline: thymic DN cells from donor mice were adoptively transferred into congenically different 15-d-old or adult recipients. Establishment of donor-derived IELs was determined 4–5 wk later by flow cytometry. **(B and C)** Number of donor-derived small intestinal CD8αα IELs (B) or TCRγδ+ IELs (C). Each symbol represents an individual recipient. Horizontal lines in B and C indicate the median. Data are pooled from four independent experiments. *P < 0.05 and ****P < 0.0001 (Mann-Whitney test).

had high expression of $\alpha_4\beta_7$ (Fig. 3, F and G). Taken together, our data indicate that at an age at which IELps abundantly seed the gut, type B IELps have an emigration-competent and mucosal-homing phenotype. With progressing age, these characteristics became confined to type A IELps.

Time-stamp labeling reveals distinct TCR Vα usage in developmentally early CD8αα IELs

Since the thymic type B IELp phenotype indicated similar thymic emigration and mucosal homing capacities as type A IELps in young mice, we wanted to get further clues as to whether this advantage was reflected in the intestinal IEL composition. Contrary to the thymic precursors, type A– and type B–derived IELs have no known markers that can be used to distinguish them, and direct fate mapping of type A and B IELps is not possible to date. However, we previously found an enrichment of specific TCR Vα chains in each population—Vα2 for type A and Vα3.2 for type B IELps (Ruscher et al., 2017)—and therefore analyzed Vα usage in time-stamp–labeled IELs. We first confirmed that, similar to those of adult mice, thymic type A IELps were biased toward TCR Vα2+ cells and type B toward TCR Vα3.2+ in young mice (Fig. 4, A and B; Ruscher et al., 2017). Intriguingly, CD8αα IELs that were time-stamp labeled in early life showed a preference for Vα3.2 expression that waned as animals approached adulthood (Fig. 4 C). These data are in agreement with the thymus emigration-competent and greater mucosal-homing phenotype of type B compared with type A IELps in young mice (as established in Fig. 3). The combined results suggest that the equal proportions of Vα2+ and Vα3.2+ gut IELs in adult mice (Fig. 4 D) reflect a preferential seeding of Vα3.2+ cells early in life and (relatively slow) seeding of Va2+ cells that continues throughout adult life.

CD8αα IELs are less reliant on their antigen receptor for survival than are conventional IELs

Although CD8αα IELs have a memory phenotype, we do not know much about their life span. Our time-stamp data indicated that both CD8αα and CD8αβ IELs established in early life reside in the gut for at least 5 wk. We were interested in survival signals necessary for the maintenance of these cells, specifically the role of their antigen receptor. CD8αα IELs were shown to possess TCRs that predetermine their fate (McDonald et al., 2014). It is likely that thymic events such as chemokine receptor expression, retention versus egress, and survival versus deletion are driven by TCR signaling. Whether established IELs rely on antigen receptor stimulation for their maintenance, however, or merely use their TCR as a "ticket to the gut" is still an open question.

To investigate the extent to which IELs rely on survival signals through their antigen receptors, we pursued an approach that directly eliminates the TCRαβ complex in IELs. We generated UBC^{CreERT2}×TCR C$\alpha^{fl/fl}$ mice, in which administration of tamoxifen excises the Cα gene and therefore permanently ablates cell-surface TCR expression. Since gene and protein expression of the TCRβ chain is not affected by this approach, T cells would still be identifiable by intracellular TCRβ staining. To test our system, we first analyzed T cells in the blood that were surface stained with one fluorochrome-conjugated antibody to TCRβ, then intracellularly stained using a different fluorochrome. 7 d after tamoxifen administration, all CD8+ cells were positive for intracellular TCRβ, while a large fraction of these cells was negative for surface TCRβ (Fig. 5 A). We then analyzed IELs at 7 d and 21 d after tamoxifen. Surface TCR staining was eliminated from 60% of CD8αβ and CD8αα IELs 7 d after injecting tamoxifen (Fig. 5, B and C). Interestingly, however, the CD8αβ IEL population consisted largely of surface TCR+ cells by 21 d (Fig. 5 B), while a large fraction of CD8αα IELs remained surface TCR negative (Fig. 5 C). This difference was observed despite unchanged total numbers of either IEL population at days 7 or 21 (Fig. 5, D and E).

These results indicate that CD8αα IELs have a lower reliance on antigen receptor signals for their survival and/or retention. Future studies will be necessary to elucidate whether the TCR of these cells has any function beyond imprinting their fate to become CD8αα IELs.

Together, our results indicate that CD8αα IELs are predominantly established within the first 3 wk of life. Our data suggest a model wherein there is rapid establishment of type B IELp-derived CD8αα IELs (Fig. 5 F). This early dominance of type B–derived IELs, however, gets steadily diluted by a slow but constant entry of type A IELp-derived CD8αα IELs. Our findings and the observation that adult animals appear to have predominantly type A IELp-derived CD8αα IELs (McDonald et al., 2014) suggest that indeed the type A IELp-derived cells may eventually outcompete the early-established type B IELp-derived CD8αα IELs (Fig. 5 F). How this process is regulated will be important to establish in follow-up studies. Factors may include availability of IL-15 or genes regulated by the transcription factor c-Myc (Hummel et al., 2020).

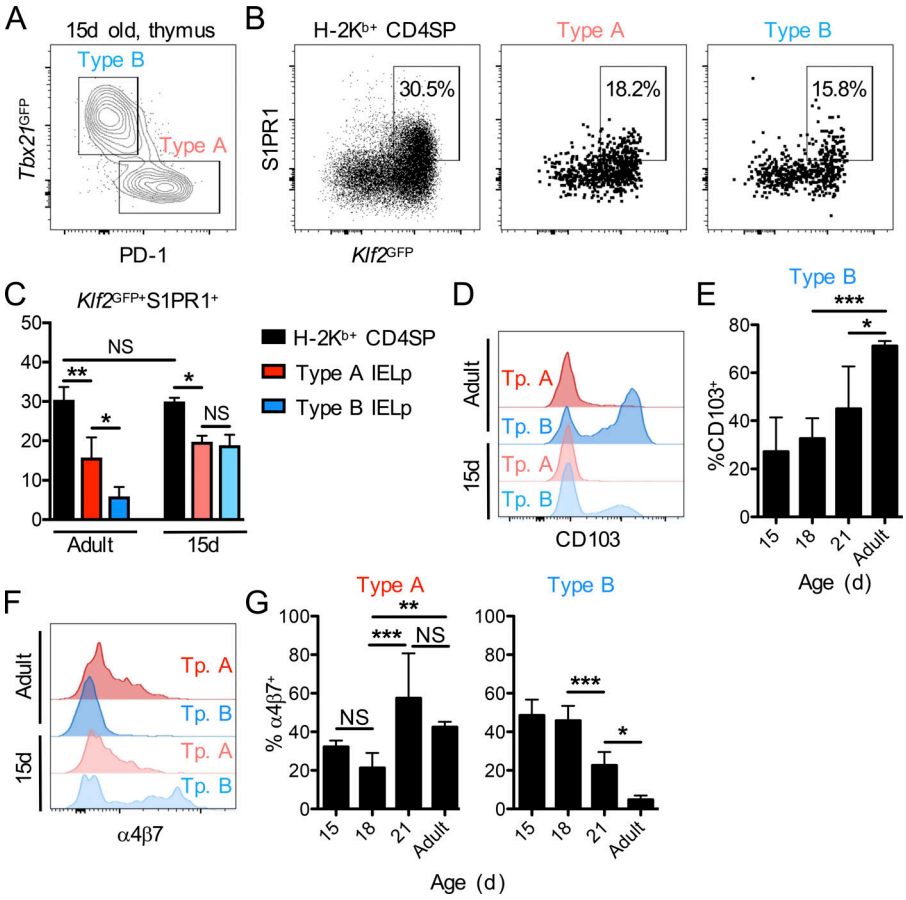

Figure 3. **Type B IELps have a thymus-emigrating phenotype in early life. (A)** Flow cytometry for PD-1 and *Tbx21*^{GFP} within CD25^{-}CD1dtet^{-}TCRβ^{+}CD5^{+} DN thymocytes for the identification of type A (PD-1^{+}*Tbx21*$^{GFP-}$; red) and type B (PD-1^{-}*Tbx21*$^{GFP+}$; blue) IELps in 15-d-old *Tbx21*^{GFP} mice. **(B and C)** Thymic H-2K^{b+} (mature) CD4SP cells and type A (PD-1^{+}; red) or type B (PD-1^{-}; blue) IELps of 15-d-old *Klf2*^{GFP} mice were analyzed for GFP and S1PR1 expression by flow cytometry (B), and the frequency of *Klf2*$^{GFP+}$S1PR1^{+} cells was summarized (n = 3; C). **(D–G)** Type A (PD-1^{+}*Tbx21*$^{GFP-}$; red) and type B (PD-1^{-}*Tbx21*$^{GFP+}$; blue) IELps in 15- (n = 4–7), 18- (n = 8 or 9), or 21- (n = 3–5) day-old or adult (n = 3–5) *Tbx21*^{GFP} mice were analyzed for surface expression of CD103 and α4β7. The expression levels in 15-d-old versus adult animals are shown as histograms (D and F), while the bar graphs depict the frequencies of CD103^{+} type B IELps (E) or α4β7^{+} type A and type B IELps (G). Data in C, E, and G are pooled from at least three independent experiments and show the mean ± SD. *P < 0.05, **P < 0.01, and ***P < 0.001 (ANOVA with Bonferroni post-test in C, E, and G). Tp., type.

What could be the reason for such differences between young and adult mice? CD8αα IELs are known to be heterogeneous in terms of their restriction to MHC molecules (Mayans et al., 2014; McDonald et al., 2014; Ruscher et al., 2017), indicating a potential variability in functions that individual subsets of these cells carry out. It is intriguing to speculate that the composition of this cell population is dynamic and could carry out different roles with age. Availability of antigen in the gastrointestinal tract is subject to dramatic changes between birth and weaning: the transition in diet from milk to solid food occurs in this period, and colonization of the gut with biota rapidly increases from 2 wk of age onward (Knoop et al., 2017; Koenig et al., 2011). There may therefore be a greater demand for IELs reactive to foreign antigens in the gut at this stage in life, when the intestinal immune system is still relatively naive. This would be in line with our previous finding that unlike type A IELps, type B IELps are not obviously self-reactive (Ruscher et al., 2017). IELs derived from self-reactive type A IELps may scan the epithelium for cancerous cells, as previously suggested (Cheroutre et al., 2011). Alternatively, they may not have an antigen receptor–specific function at all. Although direct functional studies are currently impossible due to the lack of specific markers that discriminate type A and type B IELp-derived CD8αα IELs, future studies ought to establish specific genetic markers for type A and B IELps to test this model using genetic fate mapping. Indeed, there is precedence for a special role of microbiota-recognizing unconventional T cells in early life at barrier tissues. For example, one study highlighted the existence of an early wave of commensal-specific T reg cells migrating to the skin, which are functionally different from T reg cells occupying this site later in life (Scharschmidt et al., 2015). Another publication reported the relevance of microbiota recognition by T reg cells in the neonatal lung for tolerance to allergens in later life (Gollwitzer et al., 2014).

In summary, we report unexpected seeding kinetics of unconventional CD8αα IELs mostly confined to a tight time window in the first weeks of life. We further provide evidence supporting a preference for Vα3.2^{+} CD8αα IELs in postnatal life, which is lost at later stages. In addition, CD8αα and CD8αβ IELs in adult animals showed surprising differences in population dynamics upon ablation of their antigen receptor. These findings provide novel insight into the kinetics of IEL establishment as well as its maintenance and contribute to our understanding of these abundant populations of barrier surface T cells.

Materials and methods

Mice

Cd4^{CreERT2} and *Rosa26*^{tdT} mice were purchased from Jackson Laboratories. C57BL/6 and B6.SJL mice were obtained from the National Cancer Institute. Tbet^{GFP} (*Tbx21*^{GFP}/*Tbx21*^{ZsGreen}) and *Klf2*^{GFP} mice were described previously (Weinreich et al., 2009; Zhu et al., 2012). TCR Cα$^{fl/fl}$ mice were a kind gift from the Alexander Rudensky group (Memorial Sloan Kettering Cancer

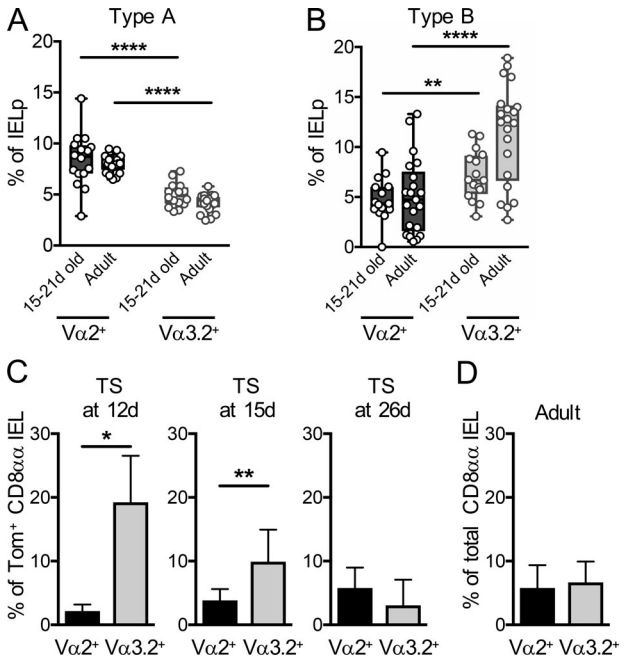

Figure 4. **Distinct TCR Vα usage in CD8αα IELs time-stamped in early life. (A and B)** Type A (A) and type B (B) IELps were analyzed by flow cytometry for expression of the TCR Vα2 and Vα3.2 chains in 15–21-d-old and adult *Tbx21*^{GFP} or C57BL/6 mice. **(C)** *Cd4*^{CreERT2}×*Rosa26*^{tdT} mice were time-stamped by intraperitoneal injection of tamoxifen or 4-OHT at various ages. Time-stamp–labeled Tomato$^+$ small intestinal CD8αα IELs were analyzed 4–5 wk later by flow cytometry for expression of Vα2 and Vα3.2. (n = 3 [12 d and 26 d]; n = 8 [15 d]). **(D)** *Cd4*^{CreERT2}×*Rosa26*^{tdT} mice were time-stamped by intraperitoneal injection of 4-OHT at ages between 10 and 15 d. 4–5 wk later, the total combined Tomato$^+$ and Tomato$^-$ small intestinal CD8αα IELs were analyzed for expression of Vα2 and Vα3.2 (n = 9). Each symbol in A and B represents an individual recipient, and the graphs are pooled from 10 independent experiments; they show median (center lines) with 25th and 75th percentiles (box limits). The whiskers indicate the smallest and largest values. Data in C and D are pooled from at least two independent experiments and show the mean ± SD. *P < 0.05, **P < 0.01, and ****P < 0.0001 (Student's t test). TS, time-stamped.

Center, New York, NY) and have been described previously (Polic et al., 2001). TCR Cα$^{fl/fl}$ mice were backcrossed to UBC^{CreERT2} mice (Jackson Laboratories) to generate UBC^{CreERT2}×TCR Cα$^{fl/fl}$ mice. All mice were on a C57BL/6 genetic background, and colonies were bred at the University of Minnesota Center for Immunology animal housing facilities to obtain mice of various ages. Young mice were aged as indicated in the corresponding figures/text, while adult mice were between 6 and 16 wk old. Animal experiments were approved by the Institutional Animal Care and Use Committee of the University of Minnesota.

Time-stamp fate mapping

Cd4^{CreERT2} mice were crossed with *Rosa26*^{tdT} mice. The offspring were injected intraperitoneally at the indicated ages with either 4-OHT (Sigma-Aldrich) at ages 5–15 d or tamoxifen (Sigma-Aldrich) at ages 21 d and older, in sunflower oil 2% EtOH at 100 µg per gram mouse weight. The thymus, spleen, or small intestinal IELs were analyzed on various days after injection (as indicated in figures and text).

IEL isolation

IELs were isolated as follows: small intestines were cleaned of feces and mucus, Peyer's patches were removed, and the remaining tissue was cut into ∼0.5-cm-long pieces. The tissues were then incubated for 30 min in HBSS (without Ca^{++} and Mg^{++}) 1 mM dithiothreitol, 5 mM EDTA, and 5% FBS at 37°C in a shaking incubator (200–250 rpm). IELs were obtained by filtering through 70-µm strainers. IELs from mice over 15 d of age were further cleaned up by Percoll density gradient centrifugation as explained in Ruscher et al. (2017).

Flow cytometry

Single-cell suspensions of thymus, spleen, or small intestinal IELs were labeled with antibodies purchased from Biolegend, eBioscience, R&D Systems, or Tonbo. IELs were identified as live singlet TCRγδ$^+$ (TCRγδ IEL), or TCRβ$^+$CD4$^-$CD8α$^+$CD8β$^-$ (CD8αα IEL), or TCRβ$^+$CD4$^-$CD8α$^+$CD8β$^+$ (CD8αβ IEL) as in Ruscher et al. (2017). Mature thymic IELps were identified as singlet CD1dtet$^-$CD25$^-$CD4$^-$CD8$^-$CD5$^+$TCRβ$^+$CD122$^+$H-2K^{b+} cells as in Ruscher et al. (2017). Clones were CD4 (RM4-5), CD8α (53–6.7), CD8β (53–5.8), CD103 (M290), TCRβ (H57-597), TCRγδ (GL3), H-2K^b (AF6-88.5), CD5 (53–7.3), CD25 (PC61), PD-1 (J43), CD122 (TM-b1), α4β7 (DATK32), Vα2 (B20.1), Vα3.2 (RR3-16), Ki67 (16A8), CD45.1 (A20), and CD45.2 (104). CD1d fluorochrome-labeled tetramers (CD1d^{tet}) were obtained by incubating biotinylated CD1d/PBS57 monomers (National Institutes of Health) with Streptavidin PE, APC, or PE/Cy7. Cells were stained on ice for 20 min. S1PR1 staining was performed as described previously (Ruscher et al., 2017). Cell numbers were established using AccuCheck counting beads (Invitrogen/Life Technologies).

Adoptive transfers

Thymic DN was isolated from thymi of adult B6.SJL mice by depletion of CD8$^+$ and CD4$^+$ cells by MACS (Miltenyi). The procedure was repeated to obtain a purity of >98% DN cells. 200,000–700,000 DN cells were transferred by retro-orbital intravenous injection into either CD45.1/2$^+$ or CD45.2$^+$ 15-d-old or adult recipients and recovered 4–5 wk later. For interexperimental comparison, the recovered cell numbers were normalized to 10^6 transferred cells.

Surface TCR depletion

TCR Cα$^{fl/fl}$ mice were injected with tamoxifen (Sigma-Aldrich) in sunflower oil 2% EtOH at 300 µg per gram mouse weight or 6 mg/mouse. The small intestinal IELs were analyzed on various days after injection (as indicated in the figures and text).

Statistical analysis

Data were analyzed and arranged using GraphPad Prism versions 6.0 and 7.0. Unpaired Student's t test or nonparametric Mann-Whitney test was used to compare two datasets, and one-way ANOVA with Bonferroni post-test was performed for comparison of three or more datasets. Sample size, experimental replicates, and statistical method used are explained in each figure legend.

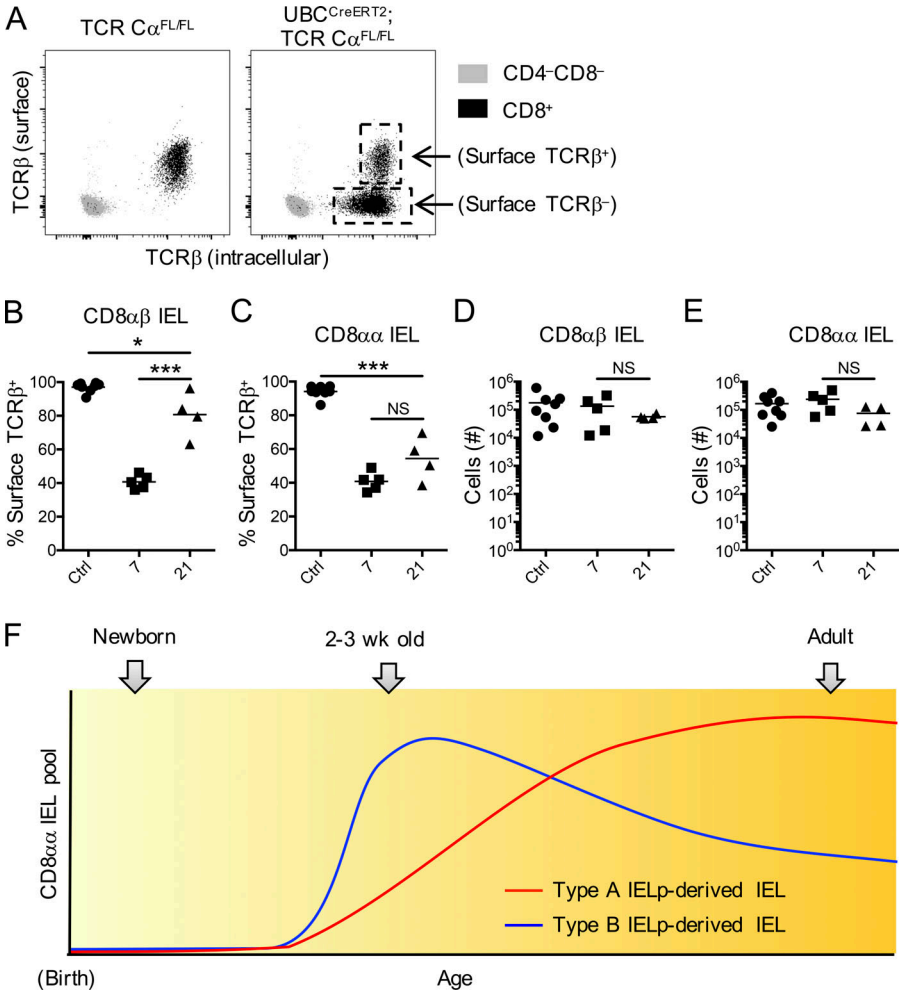

Figure 5. **Reliance on TCR for IEL maintenance. (A)** Representative plots of peripheral blood samples taken from TCR $C\alpha^{fl/fl}$ (left plot, control) or $UBC^{CreERT2}$×TCR $C\alpha^{fl/fl}$ mice (right plot) 7 d after administration of tamoxifen. The samples were surface stained for CD4 and CD8 and surface stained with one fluorochrome-conjugated antibody to TCRβ, then intracellularly stained with another. Shown are $CD4^-CD8^-$ cells (gray) and $CD8^+$ T cells (black). **(B–E)** Frequency of surface $TCR\beta^+$ within total (surface and intracellular) $TCR\beta^+$ CD8αβ IELs (B) or CD8αα IELs (C) and numbers of total CD8αβ IELs (D) and CD8αα IELs (E) in the small intestine of TCR $C\alpha^{fl/fl}$ (control) and $UBC^{CreERT2}$×TCR $C\alpha^{fl/fl}$ (sample) mice. **(F)** Proposed model for CD8αα IEL establishment. Each symbol in B–E represents an individual mouse. Horizontal lines indicate the mean. Data are pooled from eight independent experiments. *P < 0.05 and ***P < 0.001 (ANOVA with Bonferroni post-test).

Online supplemental material

Fig. S1 and Fig. S2 relate to Fig. 1 and to the subsection Time-stamping a wave of IELps in adult and neonatal mice. Fig. S1 shows the number of $TCR\alpha\beta^+CD4^-$ CD8αα and CD8αβ IELs in the small intestine at the ages of 15 d, 20 d, and 5–9 wk, while Fig. S2 shows the labeling kinetics of time-stamped cells in the thymus. Fig. S3 A relates to Fig. 1 and indicates the gating strategy for $tdTomato^+$ IELs. Fig. S3 B relates to Fig. 3 and shows the gating strategy for mature thymic IELps.

Acknowledgments

The authors thank J. Ding for technical assistance. We further thank Dr. Hristo Georgiev for reading the manuscript and providing feedback and suggestions.

This work was supported by National Institutes of Health grants R37 AI39560 and PO1 AI35296 to K.A. Hogquist.

Author contributions: R. Ruscher and K.A. Hogquist designed the experiments, conceptualized the study, and wrote the manuscript. The majority of the experiments and analysis were performed by R. Ruscher, while S.T. Lee, O.C. Salgado, E.R. Breed, and S.H. Osum substantially contributed to some experiments and to drafting the work.

Disclosures: The authors declare no competing interests exist.

Submitted: 17 December 2019
Revised: 27 April 2020
Accepted: 12 June 2020

References

Berlin, C., E.L. Berg, M.J. Briskin, D.P. Andrew, P.J. Kilshaw, B. Holzmann, I.L. Weissman, A. Hamann, and E.C. Butcher. 1993. Alpha 4 beta 7 integrin mediates lymphocyte binding to the mucosal vascular addressin MAdCAM-1. *Cell*. 74:185–195. https://doi.org/10.1016/0092-8674(93)90305-A

Carlson, C.M., B.T. Endrizzi, J. Wu, X. Ding, M.A. Weinreich, E.R. Walsh, M.A. Wani, J.B. Lingrel, K.A. Hogquist, and S.C. Jameson. 2006. Kruppel-like factor 2 regulates thymocyte and T-cell migration. *Nature*. 442:299–302. https://doi.org/10.1038/nature04882

Cepek, K.L., S.K. Shaw, C.M. Parker, G.J. Russell, J.S. Morrow, D.L. Rimm, and M.B. Brenner. 1994. Adhesion between epithelial cells and T lymphocytes mediated by E-cadherin and the α E beta 7 integrin. *Nature*. 372:190–193. https://doi.org/10.1038/372190a0

Cheroutre, H., F. Lambolez, and D. Mucida. 2011. The light and dark sides of intestinal intraepithelial lymphocytes. *Nat. Rev. Immunol.* 11:445–456. https://doi.org/10.1038/nri3007

Gangadharan, D., F. Lambolez, A. Attinger, Y. Wang-Zhu, B.A. Sullivan, and H. Cheroutre. 2006. Identification of pre- and postselection TCRalphabeta+ intraepithelial lymphocyte precursors in the thymus. *Immunity*. 25:631–641. https://doi.org/10.1016/j.immuni.2006.08.018

Golec, D.P., R.E. Hoeppli, L.M. Henao Caviedes, J. McCann, M.K. Levings, and T.A. Baldwin. 2017. Thymic progenitors of $TCR\alpha\beta^+$ CD8αα intestinal intraepithelial lymphocytes require RasGRP1 for development. *J. Exp. Med.* 214:2421–2435. https://doi.org/10.1084/jem.20170844

Gollwitzer, E.S., S. Saglani, A. Trompette, K. Yadava, R. Sherburn, K.D. McCoy, L.P. Nicod, C.M. Lloyd, and B.J. Marsland. 2014. Lung microbiota promotes tolerance to allergens in neonates via PD-L1. *Nat. Med.* 20: 642–647. https://doi.org/10.1038/nm.3568

Guy-Grand, D., P. Vassalli, G. Eberl, P. Pereira, O. Burlen-Defranoux, F. Lemaitre, J.P. Di Santo, A.A. Freitas, A. Cumano, and A. Bandeira. 2013. Origin, trafficking, and intraepithelial fate of gut-tropic T cells. *J. Exp. Med.* 210:1839–1854. https://doi.org/10.1084/jem.20122588

Hamann, A., D.P. Andrew, D. Jablonski-Westrich, B. Holzmann, and E.C. Butcher. 1994. Role of alpha 4-integrins in lymphocyte homing to mucosal tissues in vivo. *J. Immunol.* 152:3282–3293.

He, S., F. Kahles, S. Rattik, M. Nairz, C.S. McAlpine, A. Anzai, D. Selgrade, A.M. Fenn, C.T. Chan, J.E. Mindur, et al. 2019. Gut intraepithelial T cells calibrate metabolism and accelerate cardiovascular disease. *Nature.* 566: 115–119. https://doi.org/10.1038/s41586-018-0849-9

Hoytema van Konijnenburg, D.P., B.S. Reis, V.A. Pedicord, J. Farache, G.D. Victora, and D. Mucida. 2017. Intestinal Epithelial and Intraepithelial T Cell Crosstalk Mediates a Dynamic Response to Infection. *Cell.* 171: 783–794.e13: E13. https://doi.org/10.1016/j.cell.2017.08.046

Hummel, J.F., P. Zeis, K. Ebert, J. Fixemer, P. Konrad, C. Schachtrup, S.J. Arnold, D. Grün, and Y. Tanriver. 2020. Single-cell RNA-sequencing identifies the developmental trajectory of C-Myc-dependent NK1.1^{-} T-bet^{+} intraepithelial lymphocyte precursors. *Mucosal Immunol.* 13: 257–270. https://doi.org/10.1038/s41385-019-0220-y

Klose, C.S.N., J.F. Hummel, L. Faller, Y. d'Hargues, K. Ebert, and Y. Tanriver. 2018. A committed postselection precursor to natural TCRαβ^{+} intraepithelial lymphocytes. *Mucosal Immunol.* 11:333–344. https://doi.org/10.1038/mi.2017.54

Knoop, K.A., J.K. Gustafsson, K.G. McDonald, D.H. Kulkarni, P.E. Coughlin, S. McCrate, D. Kim, C.S. Hsieh, S.P. Hogan, C.O. Elson, et al. 2017. Microbial antigen encounter during a preweaning interval is critical for tolerance to gut bacteria. *Sci. Immunol.* 2. eaao1314. https://doi.org/10.1126/sciimmunol.aao1314

Koenig, J.E., A. Spor, N. Scalfone, A.D. Fricker, J. Stombaugh, R. Knight, L.T. Angenent, and R.E. Ley. 2011. Succession of microbial consortia in the developing infant gut microbiome. *Proc. Natl. Acad. Sci. USA.* 108(Suppl 1):4578–4585. https://doi.org/10.1073/pnas.1000081107

Kuo, S., A. El Guindy, C.M. Panwala, P.M. Hagan, and V. Camerini. 2001. Differential appearance of T cell subsets in the large and small intestine of neonatal mice. *Pediatr. Res.* 49:543–551. https://doi.org/10.1203/00006450-200104000-00017

Kutlesa, S., J.T. Wessels, A. Speiser, I. Steiert, C.A. Müller, and G. Klein. 2002. E-cadherin-mediated interactions of thymic epithelial cells with CD103+ thymocytes lead to enhanced thymocyte cell proliferation. *J. Cell Sci.* 115: 4505–4515. https://doi.org/10.1242/jcs.00142

Lambolez, F., M.L. Arcangeli, A.M. Joret, V. Pasqualetto, C. Cordier, J.P. Di Santo, B. Rocha, and S. Ezine. 2006. The thymus exports long-lived fully committed T cell precursors that can colonize primary lymphoid organs. *Nat. Immunol.* 7:76–82. https://doi.org/10.1038/ni1293

Matloubian, M., C.G. Lo, G. Cinamon, M.J. Lesneski, Y. Xu, V. Brinkmann, M.L. Allende, R.L. Proia, and J.G. Cyster. 2004. Lymphocyte egress from thymus and peripheral lymphoid organs is dependent on S1P receptor 1. *Nature.* 427:355–360. https://doi.org/10.1038/nature02284

Mayans, S., D. Stepniak, S. Palida, A. Larange, J. Dreux, B. Arlian, R. Shinnakasu, M. Kronenberg, H. Cheroutre, and F. Lambolez. 2014. αβT cell receptors expressed by CD4(-)CD8αβ(-) intraepithelial T cells drive their fate into a unique lineage with unusual MHC reactivities. *Immunity.* 41:207–218. https://doi.org/10.1016/j.immuni.2014.07.010

McCaughtry, T.M., M.S. Wilken, and K.A. Hogquist. 2007. Thymic emigration revisited. *J. Exp. Med.* 204:2513–2520. https://doi.org/10.1084/jem.20070601

McDonald, B.D., J.J. Bunker, I.E. Ishizuka, B. Jabri, and A. Bendelac. 2014. Elevated T cell receptor signaling identifies a thymic precursor to the TCRαβ(+)CD4(-)CD8β(-) intraepithelial lymphocyte lineage. *Immunity.* 41:219–229. https://doi.org/10.1016/j.immuni.2014.07.008

McDonald, B.D., B. Jabri, and A. Bendelac. 2018. Diverse developmental pathways of intestinal intraepithelial lymphocytes. *Nat. Rev. Immunol.* 18:514–525. https://doi.org/10.1038/s41577-018-0013-7

Pobezinsky, L.A., G.S. Angelov, X. Tai, S. Jeurling, F. Van Laethem, L. Feigenbaum, J.H. Park, and A. Singer. 2012. Clonal deletion and the fate of autoreactive thymocytes that survive negative selection. *Nat. Immunol.* 13:569–578. https://doi.org/10.1038/ni.2292

Polic, B., D. Kunkel, A. Scheffold, and K. Rajewsky. 2001. How alpha beta T cells deal with induced TCR alpha ablation. *Proc. Natl. Acad. Sci. USA.* 98:8744–8749. https://doi.org/10.1073/pnas.141218898

Ruscher, R., R.L. Kummer, Y.J. Lee, S.C. Jameson, and K.A. Hogquist. 2017. CD8αα intraepithelial lymphocytes arise from two main thymic precursors. *Nat. Immunol.* 18:771–779. https://doi.org/10.1038/ni.3751

Scharschmidt, T.C., K.S. Vasquez, H.A. Truong, S.V. Gearty, M.L. Pauli, A. Nosbaum, I.K. Gratz, M. Otto, J.J. Moon, J. Liese, et al. 2015. A Wave of Regulatory T Cells into Neonatal Skin Mediates Tolerance to Commensal Microbes. *Immunity.* 43:1011–1021. https://doi.org/10.1016/j.immuni.2015.10.016

Schön, M.P., A. Arya, E.A. Murphy, C.M. Adams, U.G. Strauch, W.W. Agace, J. Marsal, J.P. Donohue, H. Her, D.R. Beier, et al. 1999. Mucosal T lymphocyte numbers are selectively reduced in integrin alpha E (CD103)-deficient mice. *J. Immunol.* 162:6641–6649.

Smith, N.L., R.K. Patel, A. Reynaldi, J.K. Grenier, J. Wang, N.B. Watson, K. Nzingha, K.J. Yee Mon, S.A. Peng, A. Grimson, et al. 2018. Developmental Origin Governs CD8^{+} T Cell Fate Decisions during Infection. *Cell.* 174:117–130.e14: E14. https://doi.org/10.1016/j.cell.2018.05.029

Steege, J.C., W.A. Buurman, and P.P. Forget. 1997. The neonatal development of intraepithelial and lamina propria lymphocytes in the murine small intestine. *Dev. Immunol.* 5:121–128. https://doi.org/10.1155/1997/34891

Weinreich, M.A., K. Takada, C. Skon, S.L. Reiner, S.C. Jameson, and K.A. Hogquist. 2009. KLF2 transcription-factor deficiency in T cells results in unrestrained cytokine production and upregulation of bystander chemokine receptors. *Immunity.* 31:122–130. https://doi.org/10.1016/j.immuni.2009.05.011

Zhu, J., D. Jankovic, A.J. Oler, G. Wei, S. Sharma, G. Hu, L. Guo, R. Yagi, H. Yamane, G. Punkosdy, et al. 2012. The transcription factor T-bet is induced by multiple pathways and prevents an endogenous Th2 cell program during Th1 cell responses. *Immunity.* 37:660–673. https://doi.org/10.1016/j.immuni.2012.09.007

Supplemental material

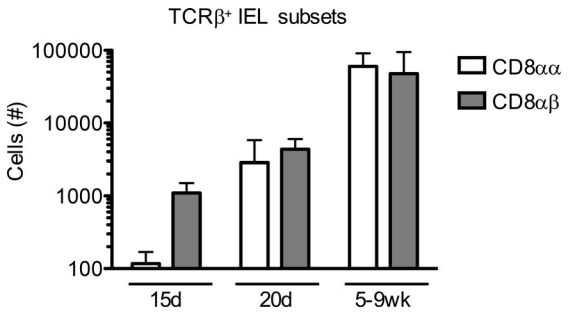

Figure S1. **IEL numbers in young and adult mice.** Small intestinal TCRαβ$^+$CD4$^-$ CD8αα and CD8αβ IELs were enumerated by flow cytometry and counting beads in mice on a C57BL/6J genetic background. Data are combined from three experiments and show the mean ± SD.

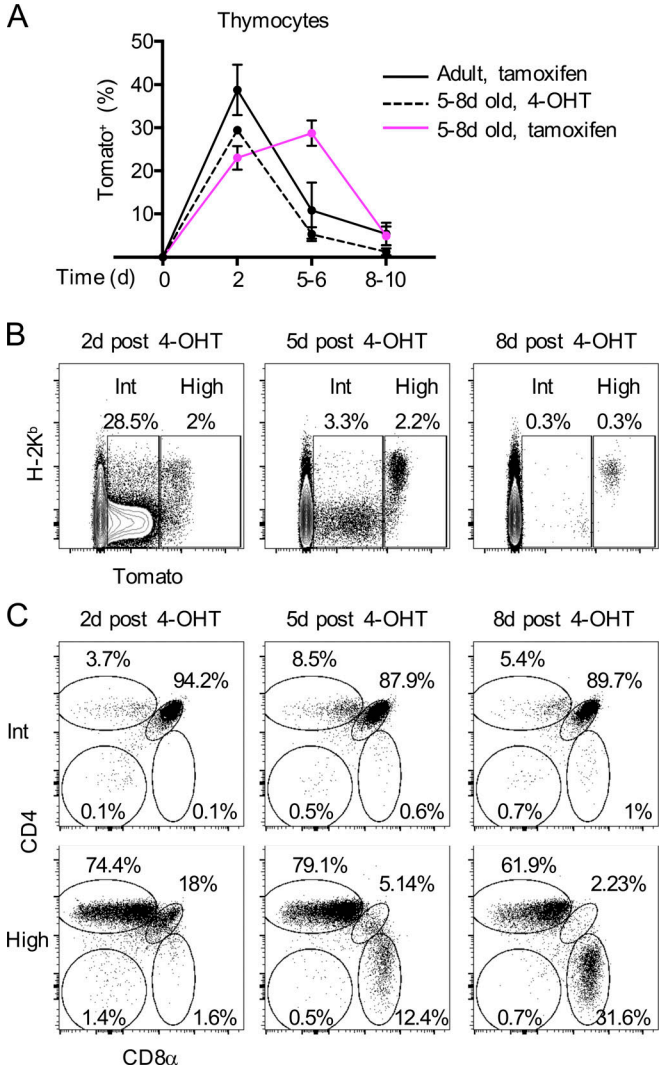

Figure S2. **Labeling kinetics of time-stamped cells in the thymus. (A)** Adult (solid black line) or 5–8-d-old (dashed line and solid pink line) stop-floxed tdTomato mice were intraperitoneally injected with tamoxifen (adult and 5–8 d old, solid pink line) or 4-OHT (5–8 d old, dashed line). The proportion of Tomato$^+$ thymocytes was analyzed by flow cytometry 2, 5–6, and 8–10 d later. **(B and C)** 7-d-old stop-floxed tdTomato mice were injected with 4-OHT. **(B)** Plots showing Tomato label versus the maturation marker H-2K^b 2 d, 5 d, and 8 d after 4-OHT administration. **(C)** Cells within the Tomato^{Int} and Tomato^{High} fractions in A were plotted as CD4 versus CD8α. Data in A are combined from two independent experiments and show the mean ± SEM. Plots in B and C are representative of a minimum of two independent experiments.

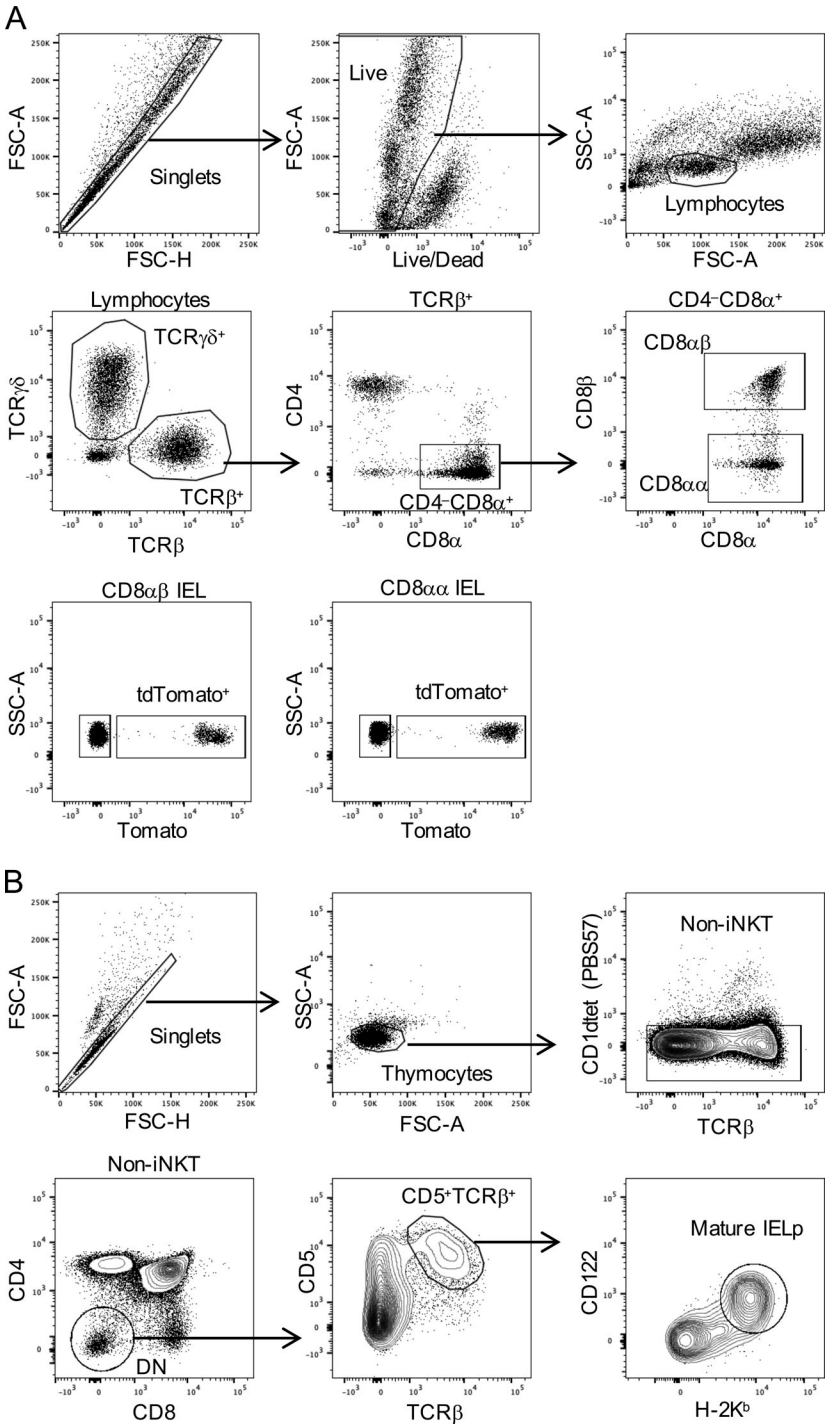

Figure S3. **Gating strategy for tdTomato⁺ IELs and for mature thymic IELps. (A)** Shown are representative plots of small-intestinal IELs from a *Cd4*^{CreERT2}×*Rosa26*^{tdT} mouse that was time-stamped at 12 d of age, as explained in Fig. 1. **(B)** Shown are representative plots of thymocytes from a 21-d-old *Tbx21*^{GFP} mouse. Data are representative of at least two independent experiments. FSC-A, forward scatter area; FSC-H, forward scatter height; iNKT, invariant natural killer T cells; SSC-A, side scatter area.